OXFORD

Anxiety disrupts performance monitoring: integrating behavioral, event-related potential, EEG microstate, and sLORETA evidence

Kyle Nash [iD][1,*], Josh Leota[2], Tobias Kleinert[1,3], Dana A. Hayward[1]

[1]Department of Psychology, University of Alberta, P-217 Biological Sciences Building, Edmonton, AB T6G 2R3, Canada,
[2]School of Psychological Sciences, Turner Institute for Brain and Mental Health, Monash University, Melbourne, VIC, 3168, Australia,
[3]Department of Ergonomics, Leibniz Research Centre for Working Environment and Human Factors, Ardeystr. 67, 44139 Dortmund, Germany
*Corresponding author: University of Alberta, P-217 Biological Sciences Building, Edmonton, AB T6G 2R3, Canada. Email: knash@ualberta.ca

Anxiety impacts performance monitoring, though theory and past research are split on how and for whom. However, past research has often examined either trait anxiety in isolation or task-dependent state anxiety and has indexed event-related potential components, such as the error-related negativity or post-error positivity (Pe), calculated at a single node during a limited window of time. We introduced 2 key novelties to this electroencephalography research to examine the link between anxiety and performance monitoring: (i) we manipulated antecedent, task-independent, state anxiety to better establish the causal effect; (ii) we conducted moderation analyses to determine how state and trait anxiety interact to impact performance monitoring processes. Additionally, we extended upon previous work by using a microstate analysis approach to isolate and sequence the neural networks and rapid mental processes in response to error commission. Results showed that state anxiety disrupts response accuracy in the Stroop task and error-related neural processes, primarily during a Pe-related microstate. Source localization shows that this disruption involves reduced activation in the dorsal anterior cingulate cortex and compensatory activation in the right lateral prefrontal cortex, particularly among people high in trait anxiety. We conclude that antecedent anxiety is largely disruptive to performance monitoring.

Key words: anxiety; EEG; performance monitoring; microstates; anterior cingulate cortex.

Introduction

Performance monitoring is essential to an organism's survival in rapidly changing and complex environments. Across cybernetic models of self-regulation, a comparator function is described in which current behavior is evaluated against a standard or goal target to prompt the organism to either continue to progress toward or adjust behavior to better pursue a desired outcome (e.g. Carver and Scheier 2001). A substantial literature links this comparator function to a dorsal anterior cingulate cortex (dACC)–lateral prefrontal cortex (PFC) neural circuit (Hauser et al. 2014; Ito et al. 2003; Paus 2001; Shackman et al. 2011), in which the dACC detects conflict and discrepancy and engages the lateral PFC for conflict resolution and behavioral modification (MacDonald et al. 2000; Miller and Cohen 2001; Botvinick et al. 2004; Yeung et al. 2004; Mansouri et al. 2009). Notably, mood disorders have been reliably associated with disrupted or impaired performance monitoring processes and functional and structural differences in the dACC and lateral PFC (Pujol et al. 2002; Olvet and Hajcak 2008; Duval et al. 2015), further demonstrating the importance of performance monitoring in healthy functioning. Past research on performance monitoring has heavily focused on links with anxiety. However, despite the heavy focus, prior

research has not been able to determine how, when, and for whom anxiety impacts performance monitoring. In the present study, we induced antecedent state anxiety via an economic anxiety (vs. no-anxiety control) manipulation and used a microstate approach to identify and sequence the mental processes involved in performance monitoring in a subsequent color-naming Stroop task.

Traditionally, there have been 2 opposing ideas regarding how anxiety influences performance monitoring that may be broadly construed as "cognitive" and "motivational" views. According to a cognitive view, anxiety is thought to be disruptive. Performance monitoring requires cognitive control and anxiety strips resources away from cognitive control (Eysenck and Derakshan 2011). According to a motivational view, anxiety is thought to be facilitative. Anxiety heightens sensitivity to aversive stimuli, and error commission is an aversive event (e.g. Hajcak and Foti 2008). Much like these opposing views, research is similarly conflicting, sometimes supporting a cognitive–disruptive account (e.g. Moser et al. 2005; Aarts and Pourtois 2012; Smart and Segalowitz 2017; Hsieh et al. 2021) and sometimes supporting a motivational facilitative account (Hajcak et al. 2003; Osinsky et al. 2010; Proudfit et al. 2013).

We hold that theory and literature are unable to separate these opposing views for 3 primary reasons. First, past research has often relied on putative anxiety manipulations administered during the task of interest (e.g. Jackson et al. 2015). However, anxiety manipulated during a cognitive task may affect performance via a mechanism similar to those in divided attention tasks, in which additional, and often irrelevant, task elements distract and impair performance monitoring (e.g. Falkenstein et al. 1991). Further, these within-task manipulations presume that anxiety can be toggled on and off, moment to moment, from one trial to the next. However, state anxiety is known to persist, suggesting that real, within-task anxiety should spillover to subsequent trials. Additionally, certain manipulations described as anxiety-provoking may be better described as fear-provoking. Despite different antecedent conditions, different neurobiological processes, and different behavioral outcomes, both participants and researchers often conflate anxiety and fear (McNaughton and Corr 2004).

Second, past research has often indexed trait levels of anxiety (e.g. Moran et al. 2015), or sampled individuals diagnosed with anxiety disorders only (e.g. Ladouceur et al. 2006; Michael et al. 2021), and has not considered the interaction between state and trait anxiety. Trait anxiety, which refers to an individual's predisposition to the experience of anxiety (Carver and White 1994; Spielberger 1983), or diagnosed anxiety disorders say little about the actual occurrence of state anxiety, which refers to the uncomfortable emotional response of heightened arousal and vigilance that arises from uncertainty or goal conflict (Gray and McNaughton 2000), during a banal reaction time task. Instead, trait anxiety may predict performance monitoring outcomes for a variety of reasons that do not involve anxious feelings. These alternatives include developmental mechanisms (e.g. trait anxiety is associated with different developmental outcomes and abilities), a third variable (e.g. trait anxiety is associated with reduced conscientiousness), or a reverse causal process (e.g. a tendency towards poor cognitive performance leads to trait anxiety). Indeed, state and trait anxiety have been shown to have different effects on cognition (Pacheco-Unguetti et al. 2010), demonstrating that, at the very least, state anxiety cannot be the assumed mechanism among high trait anxious participants during the task of interest.

Third, past research has often focused on event-related potential (ERP) components, particularly the error-related negativity (ERN) and the post-error positivity (Pe), and has assumed that a difference in mean amplitude of the ERN or Pe reflects a difference in the intensity of error-related processing (e.g. Pasion et al. 2018). However, increased ERN amplitude has been interpreted as both more and less sensitivity to errors (Moser et al. 2013; Proudfit et al. 2013). Further, differences in amplitude may also reflect a difference in the spatial (i.e. the ERN or Pe may be strongest at different nodes across the conditions) or temporal position of

these components (i.e. the ERN or Pe may be strongest at different time points across the conditions). Finally, an ERN or Pe mean amplitude difference may also reflect a different neural process occurring at the same time.

To directly address these 3 issues, we implemented 3 specific novelties in the current research. First, we induced task-independent state anxiety to directly determine the causal effect of an anxious event on performance monitoring. Specifically, participants were randomly assigned to either a poignant, generalizable experience of economic anxiety or a comparable no-anxiety control experience, prior to the performance-monitoring task. Thus, we avoided confounds associated with a concurrent manipulation of anxiety, such as divided attention.

Second, we examined the interaction between trait and state anxiety on performance monitoring. Much like this research area in general, the link between trait anxiety and performance monitoring remains unclear. Research has shown that trait anxiety can be disruptive, facilitative, or unrelated to performance monitoring (Osinsky et al. 2010; Härpfer et al. 2020; Hsieh et al. 2021; Topor et al. 2021). As other researchers have recently noted (Seow et al. 2020), we suspect that past research appears contradictory because the association between trait anxiety and performance monitoring may be context-dependent, i.e. dependent on the interaction between trait and state anxiety. Trait anxiety may normally be facilitative as trait anxiety predisposes the individual toward heightened vigilance for negative stimuli, including error commission. However, if state anxiety is activated, then trait anxiety may be disruptive, as limited attentional resources are pulled away from the task at hand towards the broader environment. We thus performed a moderation analysis to test whether the effect of antecedent state anxiety on performance monitoring varies depending on individual differences in trait anxiety.

Third, we used a microstate approach in analyzing the full spatio-temporal EEG recorded in an ERP, allowing one to uncover and precisely sequence the neural networks and discrete and rapid mental processes. Mental processes are mediated by distributed, dynamic neural networks, and activity in these networks can be studied with millisecond precision using microstate analysis of multichannel EEG (Michel and Koenig 2018). The microstate approach has grown exponentially in popularity in recent years for studying the temporal dynamics of both resting-state (e.g. Schiller et al. 2019, 2020, 2021; Bréchet et al. 2020; da Cruz et al. 2020; de Bock et al. 2020; Nash et al. 2022) and event-related neural processing (e.g. Cacioppo et al. 2015; Schiller et al. 2016; Rohde et al. 2020; Antonova et al. 2021). By segmenting EEG recorded during a reaction time task into time periods of microstate configurations (revealed by quasi-stable scalp topographies lasting typically 50–120 ms), one can identify (and source localize) functional neural networks of the brain that each represent the implementation of a specific mental

process, all at a temporal resolution not available to other neuroimaging modalities. In capitalizing on such an integrative analysis of space and time information of EEG data, we wished to identify and sequence the mental processes involved in a color-naming Stroop task. This approach builds upon previous studies that have investigated the spatio-temporal dynamics of brain activation during the Stroop task (e.g. Khateb et al. 2000; Britz and Michel 2010; Ruggeri et al. 2019; Ménétré and Laganaro 2021) and would allow us to more precisely determine how, where, and when task-independent anxiety impacts performance monitoring processes and support either the cognitive–disruptive account, motivational facilitative account, or a novel integrative account of anxiety and performance monitoring.

Methods
Participants
Participants ($N = 110$; modal age = 19; age range = 17–26; females = 61) with normal or corrected-to-normal vision and right-handedness were recruited from a first-year psychology class and earned class credit. Based on pilot data indicating that the Economic Anxiety manipulation had a medium to large effect size on self-reported anxious uncertainty (Cohen's $d = 0.65$), and considering the degree to which anxious uncertainty would then impact electrophysiological processes and responding over time, we aimed to include 50 individuals per condition and stopped collection at the end of the 2019 fall term (power analyses in G∗Power: difference between 2 independent groups, "expected" effect size $d = 0.65$, "alpha" = 0.05, "power" = 0.80, "number of groups" = 2, "total sample size" = 60). A total of 17 participants were excluded due to poor connectivity (as indicated by impedances >10 kOhms, $n = 5$), missing EEG data ($n = 2$), or not completing the tasks ($n = 10$), leaving 93 participants (modal age = 19; age range = 17–26; females = 55) for analyses. Ethical approval for this study was provided by the University of Alberta Human Research Ethics Board (Protocol 00084513) and adheres to the principles of the Helsinki Declaration.

Procedure
All tasks were administered on Windows computers presented on a VPixx monitor using Qualtrics and Presentation software. Participants first completed an electronic informed consent, then were fitted with a 64-channel EEG headset (Brain Products) and seated at a computer station in an electrically and sound-shielded room. Participants then answered demographic questions and several personality questionnaires as part of a larger research project on individual differences in the neuroscience of self-regulation (all data available upon request). As a measure of trait anxiety, we used the well-established Behavioral Inhibition System (BIS) scale of the BISBAS scale (Carver and White 1994). Participants were then randomly assigned to either the "Economic

Anxiety" (final $n = 54$) condition or the "No-Anxiety Control" (final $n = 39$) condition. As a separate line of research, participants next completed a passive auditory oddball task (Nash et al. 2020), followed by a color-naming Stroop task (focus of the current study), and a Balloon Analogue Risk-Taking task (Nash et al. 2021; Leota, Kleinert, et al. 2021a; Leota, Nash, et al. 2021b). Next, participants rated the degree to which the Economic Anxiety manipulation made them feel a range of different positive and negative emotions, in the following order: Good, Happy, Smart, Successful, Likeable, Meaningful, Frustrated, Confused, Uncertain, Empty, Anxious, Ashamed, Insecure, Lonely, Stupid, Out of Control, and Angry (1 = Strongly Disagree, 5 = Strongly Agree). Finally, participants completed a 6-item compliance scale to measure conscientious responding (see Supplementary Materials, S1) and were debriefed, had the headset removed and hair washed, and thanked for their time.

Economic Anxiety manipulation
Participants in the Economic Anxiety condition read an ostensibly real article from CBC.ca about an unsettling economic forecast in Canada that would specifically impact young adults. The forecast was putatively compiled by top Canadian researchers who concluded that a recession was imminent and that students would be hit hardest given the vulnerable position they were left in by the 2008 economic crisis. As such, this article was tailored to participants in our sample, i.e. young students. Participants in the No-Anxiety Control condition read an ostensibly real article from CBC.ca about a more neutral economic forecast that emphasized stability and a continuation of the status quo. Notably, both forecasts were based on real, publicly available economic predictions from financial news outlets.

Stroop task
After the manipulation, participants completed a Stroop task where they were presented with color words and were asked to report via left-handed button press (keys 1–4 on a keyboard, covered in an appropriately colored sticker) the ink color of each word. As with typical Stroop tasks, half of the trials presented words that were matching or congruent across word and ink color (e.g. the word GREEN written in green ink), while the other half of trials were mismatching or incongruent across those 2 features (e.g. the word RED written in green ink). Therefore, a correct response to an incongruent trial that presented the word RED written in green ink would be to press the green colored button. Participants completed 10 practice trials, followed by 192 experimental trials, randomly intermixed to be half congruent and half incongruent. Each trial began with a fixation screen for 500 ms, followed by the stimulus presented for 200 ms. Participants had 800 ms to respond. In the practice trials, immediately following a response (or once the 800 ms window had ended), a feedback screen (indicating a "correct," "incorrect," or "too slow" response) appeared

for 500 ms, followed by a blank screen for 800 ms before the next trial began. There was no feedback given in the experimental trials, other than "too slow" feedback if the participants did not respond in the 800 ms window. Participants were instructed to respond as quickly and accurately as possible.

Mean Stroop response times (RT) for congruent and incongruent trials were calculated for each participant. Nonresponses or responses given after the 800-ms window post-stimulus presentation were coded as misses and were excluded from these RT calculations. Stroop accuracy values for congruent and incongruent trials were calculated for each participant by dividing the total number of trials (i.e. 96 per congruency type) by the number of correct responses. Finally, we examined behavioral adjustments by calculating the RT and accuracy on trials after an error or miss.

EEG recording and preprocessing

Continuous EEG was recorded using the 64 Ag-AgCl channel ActiCHamp EEG system (Brain Products), positioned according to the 10/10 system and digitized at a sampling rate of 512 Hz (24-bit precision; bandwidth: 0.1–100 Hz). During recording, signals were referenced to TP9 electrode positioned over the left mastoid. Offline, EEG was re-referenced to the average mastoids (TP9-TP10), downsampled to 256 Hz, band-pass filtered between 0.1 and 30 Hz, and notch filtered at 60 Hz. Blinks were statistically removed using the automatic ocular correction developed by Gratton et al. (1983). Artifacts were then automatically detected using the following parameters: −100 to +100 μV min/max threshold, 50 μV maximum voltage step, and 0.5 μV lowest allowed voltage (maximum–minimum) in 100-ms intervals.

ERN and Pe

EEG recordings during the Stroop Task were segmented into 1,000-ms epochs response locked on either correct or error responses, 200 ms before to 800 ms after the response. For each participant, all artifact-free epochs were then baseline-corrected by subtracting the average voltage during the −200 to −100 ms time period prior to the stimulus and averaged, creating average ERPs of correct ($M = 145.32$ trials) and error responses ($M = 46.68$ trials). On average, 6.5 error trials were removed during preprocessing due to artifacts. The ERN and correct-related negativity were defined for errors and correct responses, respectively, as the mean negative amplitude between 0 and 100 ms after stimulus at the site where the component was maximal, the fronto-central electrode FCz (see grand average ERPs in Fig. 1). Additionally, the Pe was defined where the component was maximal as the mean amplitude between 100 and 450 ms after error commission at the same FCz node.

Microstates during error commission

Group-level grand average ERP maps to error commission were computed and exported separately across participants in the Economic Anxiety and No-Anxiety control conditions. In the program CARTOOL (Brunet et al. 2011), these grand averages were entered into microstate segmentation analyses based on a spatial K-means clustering approach (random trials = 300), which uses global map dissimilarity as an index for the topographical difference between any 2 maps. Next, a topographic fitting procedure was applied to identify the most dominant topographies in the grand average ERP to error commission in both conditions. Based on prior research (e.g. Schiller et al. 2016), segmentation was conducted using the following parameters: an epoch from 101 ms before to 800 ms after response, thus excluding the portion of the ERP used in baseline correction; rejecting segments less than 5 timeframes (∼20 ms); clustering range between 3 and 10 clusters, and 300 random trials for K-means clustering. The number of 6 clusters was the optimal solution based on a metacriterion analysis in CARTOOL (Brunet et al. 2011).

The group-level clusters, or microstates, were then backfit to individual-level grand average ERPs to error commission. In this fitting procedure, each time point in the ERP is labeled with the highest correlating microstate map identified in the group-level analyses (in terms of global map dissimilarity). Individual measures of mean global field power (mGFP) were calculated for each microstate as a measure of microstate intensity.

Source localization

We used sLORETA to estimate the cortical sources of scalp-recorded activity during performance monitoring across the Economic Anxiety condition and the No-Anxiety Control condition. As opposed to dipole modeling, sLORETA computes activity as current density (A/m^2) without assuming a predefined number of active sources. The sLORETA solution space consists of 6,239 voxels (voxel size: $5 \times 5 \times 5$ mm) restricted to cortex and hippocampi, as defined by the digitized Montreal Neurological Institute (MNI) probability atlas. sLORETA has been reliably validated by research comparing sLORETA localization of EEG activity to fMRI data (Mobascher et al. 2009; Olbrich et al. 2009), positron emission tomography data (Laxton et al. 2010), and implanted electrodes in intracranial recordings (Zumsteg et al. 2006). For each participant, sLORETA images were computed for scalp-recorded activity for each timeframe across the individual-average ERP for both the correct and error responses. These images were normalized to a total current density of one and log-transformed.

Statistical analyses

Initial analyses examined if ERP mean amplitudes after error commission (i.e. the ERN and Pe) were impacted by the Economic Anxiety manipulation. We conducted independent-samples *t*-tests with the condition variable entered as the grouping variable and the ERN or Pe mean amplitude, both at FCz, as the dependent variable. Independent-samples *t*-tests were also conducted to
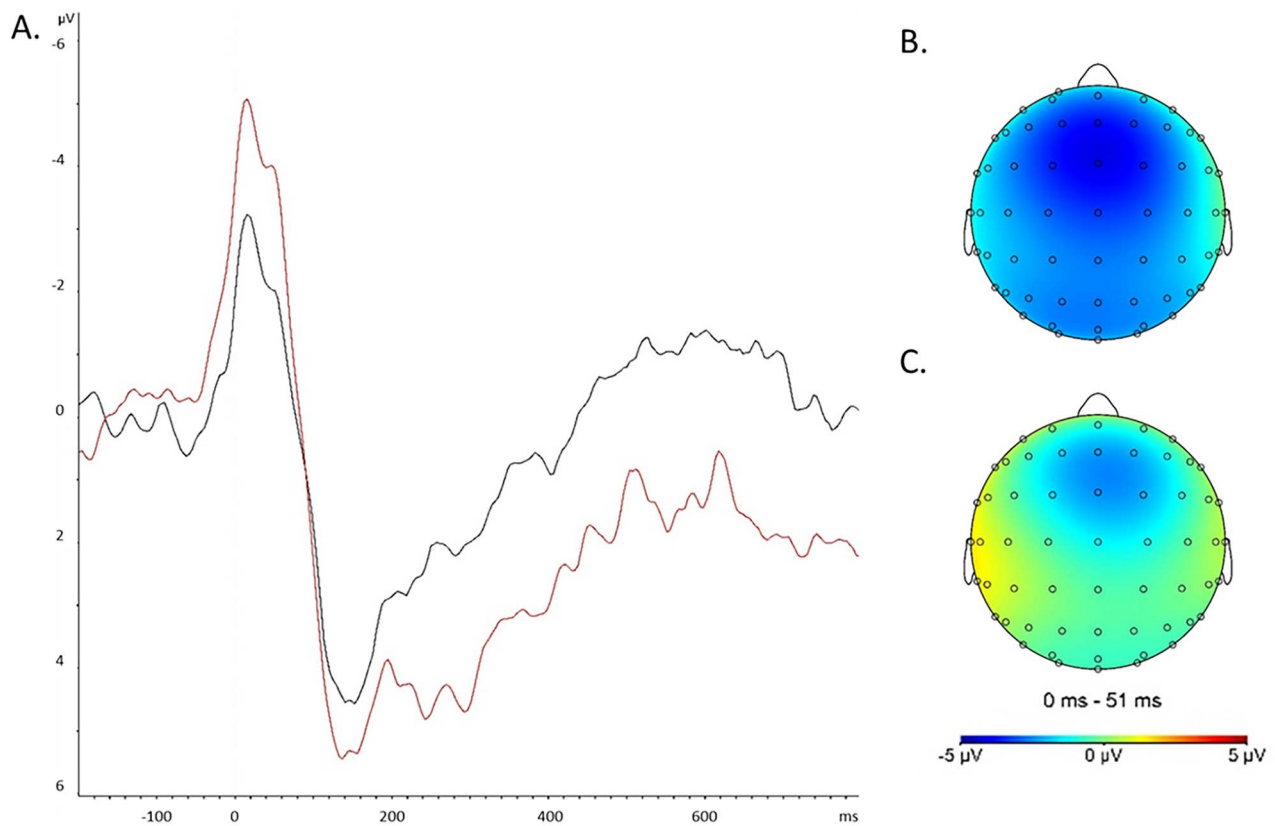
Fig. 1. A) Grand average ERP at FCz to error commission in both the Economic Anxiety (black line) and No-Anxiety Control (red line) conditions. Topography of the ERN peak at FCz in (B) No-Anxiety Control and (C) Economic Anxiety conditions (peak latencies both at 16 ms).

examine if the economic anxiety manipulation had an impact on mGFP in the microstates that were unique in the grand average ERPs, i.e. Microstates 4, 5 and 6. In order to more precisely examine neural processes in performance monitoring, we focused on (i) the paired contrast between a preceding and a subsequent microstate to source localize the sequence of cortical generators of each microstate in the 2 separate conditions, and (ii) the contrast between groups (Economic Anxiety vs. No-Anxiety Control) on error minus correct response sLORETA images during the common and unique microstates identified in the group-level analyses to determine how economic anxiety altered neural processing after error commission. In the first source localization analyses (i), whole-brain voxel-by-voxel paired sample *t*-tests of sLORETA images to error commission that were averaged across each microstate interval were conducted separately for each condition between 2 contiguous microstates, e.g. Microstate 2 difference from Microstate 1. The intervals averaged across were the same for all subjects in the same condition. Note that Microstate 1 was contrasted with the average across the preceding timeframes, corresponding to −200 to −133 ms in the ERP. Thus, we were able to sequence the intracerebral sources for each new microstate, or each step in mental processing, in each condition. In the second analyses (ii), the correct response sLORETA images were subtracted from the error sLORETA images

to remove processes common to both stimuli, allowing for more isolated focus on performance monitoring processes after error commission. Specifically, whole-brain voxel-by-voxel independent groups *t*-tests of the sLORETA images were conducted on the timeframes during the common and unique microstates (see Fig. 2), thus comparing intracerebral sources of error commission in the Economic Anxiety and the No-Anxiety Control conditions. In both analyses, correction for multiple testing for all 6,239 voxels was implemented by means of a nonparametric randomization approach (Nichols and Holmes 2002). This approach estimates empirical probability distributions and the corresponding critical probability thresholds (corrected for multiple comparisons).

We next examined if trait anxiety (measured using the BIS scale) moderated the effect of the Economic Anxiety manipulation on performance monitoring. Specifically, to examine if trait anxiety moderates the source localization effects, in MATLAB, we conducted whole-brain voxel-by-voxel moderated multiple regression tests of the sLORETA images during the identified microstate periods, with the condition variable and trait anxiety entered as first-level predictors, and their interaction term entered as a second-level predictor (MATLAB script available upon request; see West et al. 1996, for more information on analyzing categorical by continuous variables using multiple regression). Correction for
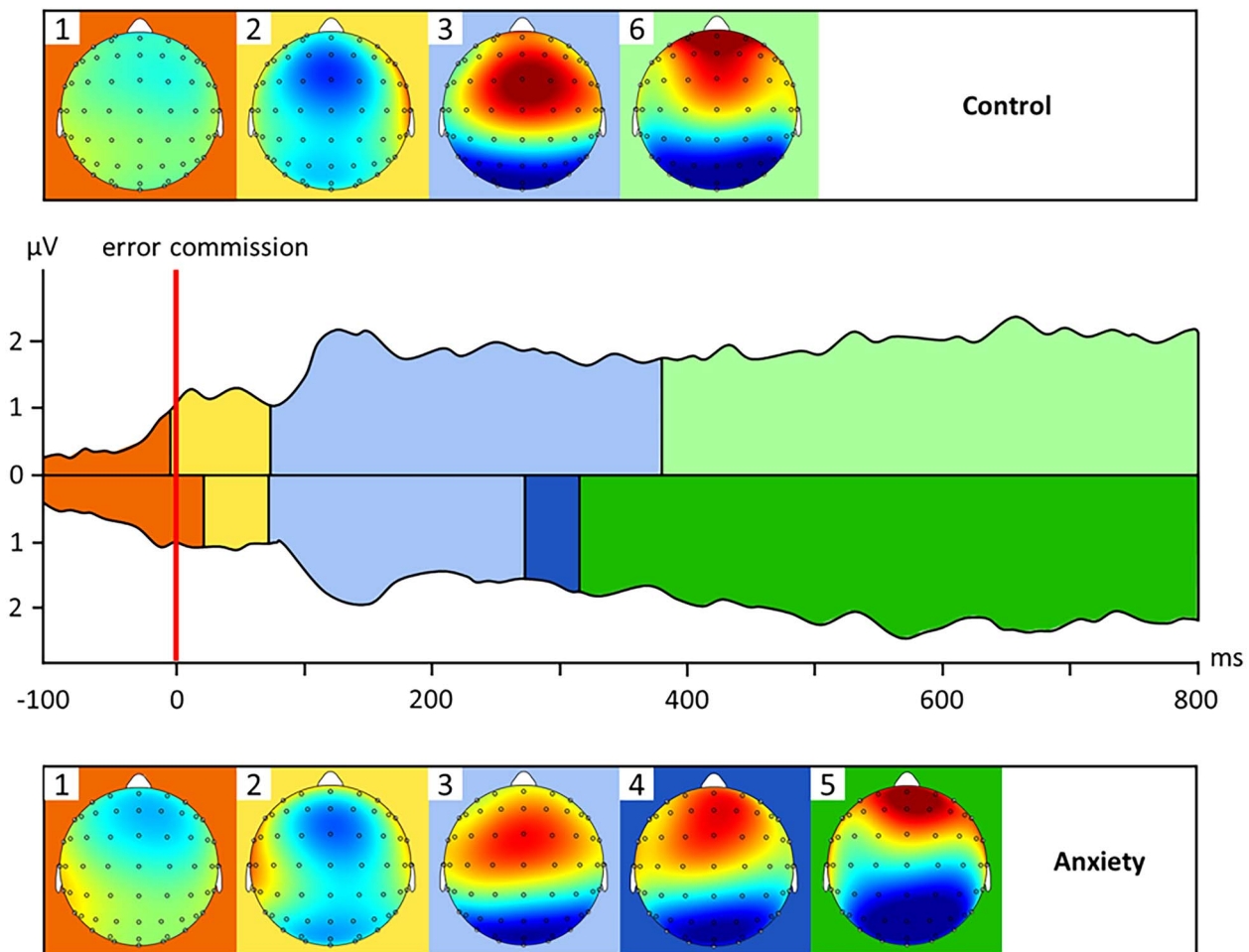
Fig. 2. Microstate sequences in response to error commission in the Stroop across time (−100 to 800 ms after stimulus presentation), for the No-Anxiety Control (top) and Economic Anxiety (bottom) conditions, plotted over the Global Field Power (GFP), with corresponding topographies for each microstate (red indicates more positive values and blue indicates more negative values, referred to an average reference).

multiple testing for all 6,239 voxels was again implemented by means of a nonparametric randomization approach (Nichols and Holmes 2002).

Results

Economic Anxiety manipulation check

Note that these manipulation check results constitute a partial reanalysis of data reported in Nash et al. (2021). We computed a State Anxiety composite (Anxious, Uncertain, and Frustrated) from the emotion scale administered as a manipulation check. In a one-way analysis of variance (ANOVA), participants in the Economic Anxiety condition reported significantly higher levels of State Anxiety ($M = 3.753$, SD $= 0.907$) than participants in the No-Anxiety Control condition ($M = 2.350$, SD $= 0.936$), $F(1, 92) = 52.710$, $P < 0.0001$, $\eta 2p = 0.367$. This demonstrates that the Economic Anxiety condition caused increased State Anxiety.

Stroop behavioral analyses

We next conducted 2 repeated-measures ANOVAs, one for RTs and one for accuracy, as a function of

"Condition" (Economic Anxiety, No-Anxiety Control) and "Congruency" (Congruent, Incongruent). The RT ANOVA returned a main effect of "Congruency," $F(1,87) = 357.118$, $P < 0.001$, with participants overall faster for congruent (521.4 ms) as compared to incongruent (567.9 ms) trials. There was no main effect of "Condition" $F(1,87) = 1.140$, $P > 0.2$, nor was there an interaction between the 2 factors ($F < 1$, $P > 0.2$). The accuracy ANOVA revealed a main effect of "Congruency," $F(1,87) = 160.405$, $P < 0.001$, with participants overall more accurate for congruent (83.3%) as compared to incongruent (68.5%) trials, as well as an interaction between "Congruency" and "Condition," $F(1,87) = 11.025$, $P = 0.001$. This interaction was driven by significantly worse performance on incongruent trials in the Economic Anxiety condition (65.1%) as compared to the No-Anxiety Control condition (71.9%), $F(1,87) = 5.374$, $P = 0.023$, with comparable accuracy for congruent trials (Economic Anxiety group: 83.8%; control group: 82.8%; $F(1,87) = 0.221$, $P = 0.639$).

We also examined the impact of an error or a miss on RT and performance in the subsequent trial. A repeated-measures ANOVA demonstrated a marginal interaction between "Condition" (Economic Anxiety,

No-Anxiety Control) and "Outcome" (Incorrect/Miss, Correct) on RT, $F(1,87) = 3.839$, $P = 0.053$. This interaction effect is statistically identical to a post-error slowing effect, and it appeared to be driven by more post-error slowing in the Economic Anxiety condition (mean RT difference Incorrect/Miss − Correct = 24.707 ms) as compared to the No-Anxiety Control condition (mean RT difference Incorrect/Miss − Correct = 12.885 ms). The same repeated-measures ANOVA demonstrated an interaction between "Condition" (Economic Anxiety, No-Anxiety Control) and "Outcome" (Incorrect/Miss, Correct) on accuracy, $F(1,87) = 4.788$, $P = 0.031$. This interaction was driven by significantly worse performance after errors or misses on the previous trial in the Economic Anxiety condition (69.2%) as compared to the No-Anxiety Control condition (77.2%), $F(1,87) = 4.708$, $P = 0.033$. Taken together, accuracy and behavioral adjustments to errors were both disrupted by the Economic Anxiety manipulation.

ERPs: ERN and Pe mean amplitude

In our initial analyses, and as seen in Fig. 1, the ERN and Pe topographies appeared muted in the Economic Anxiety versus No-Anxiety Control conditions, with the maximal ERN and Pe amplitudes at the FCz electrode, though peak latencies after error commission appeared quite similar (ERN peak: both conditions = 16 ms, Pe peak: Economic Anxiety = 152 ms, No-Anxiety Control = 137 ms). An independent samples t-test revealed that participants in the Economic Anxiety condition ($M = -1.467$, SD = 5.819), compared to participants in the No-Anxiety Control condition ($M = -3.502$, SD = 3.925), demonstrated less negative ERN mean amplitude scores at FCz, $t(90.639) = -2.013$, $P = 0.047$ (equal variances not assumed, based on Levene's test). The same analysis examining the Pe mean amplitude at FCz revealed no difference between conditions, $t(91) = 0.700$, $P = 0.486$.

Microstate analysis of error trials

We next examined the microstate sequence after error commission in the grand average ERP from both conditions. As illustrated in Fig. 2, the No-Anxiety Control condition exhibited microstates that generally correspond to typical error-related components. Microstate 1 (orange) starts at −133 ms and ends at −4 ms, near error commission, roughly corresponding with a "pre-error" component that typically precedes the ERN (Hajcak et al. 2005). Microstate 2 (yellow) starts at −4 ms and ends at 74 ms, demonstrating a strong fronto-central negativity, thus corresponding with the classic ERN (Gehring et al. 1993; Yeung et al. 2004). Microstate 3 (light blue) starts at 74 ms and ends at 379 ms, demonstrating a fronto-central positivity, thus corresponding with the Pe (Herrmann et al. 2004; Steinhauser and Yeung 2010). Finally, Microstate 6 (light green) starts at 379 ms and ends at 800 ms, the end of the ERP, demonstrating a more anterior positivity, and thus corresponding with a late

positivity potential component (Hajcak et al. 2009). On the other hand, though the Economic Anxiety condition demonstrated roughly matching early microstates (Microstate 1 = −133 to +23 ms; Microstate 2 = 23–70 ms; Microstate 3 = 70273 ms), they also produced 2 unique later microstates. Microstate 4 (dark blue) starts at 273 ms and ends at 316 ms, demonstrating a more anterior and limited fronto-central positivity compared to Microstate 3 found in the control condition in the same timeframe. Microstate 5 (dark green) starts at 316 ms and ends at 800 ms and roughly mirrors the time course and topography of Microstate 6 in the control condition, though it appears to be reduced in intensity.

The microstate templates revealed in the group-level analysis were then backfit to the individual grand average ERPs after error commission. Individual measures of mGFP were extracted for each template, as a measure of microstate intensity. We then examined if the economic anxiety manipulation had an impact on mGFP in the Microstates that were unique in the grand average ERPs, i.e. Microstates 4, 5, and 6. Independent samples t-tests showed that participants in the Economic Anxiety condition demonstrated increased mGFP for Microstate 4 ($M = 2.562$ μV^2, SD = 2.603), compared to those in the No-Anxiety control condition ($M = 1.568$ μV^2, SD = 1.837), $t(91) = -2.045$, $P = 0.044$. Similarly, participants in the Economic Anxiety condition demonstrated increased mGFP for Microstate 5 ($M = 3.273$ μV^2, SD = 2.508), compared to those in the No-Anxiety control condition ($M = 1.982$ μV^2, SD = 2.268), $t(91) = -2.549$, $P = 0.012$. There was no difference between conditions in mGFP for Microstate 6 ($P = 0.242$). In sum, these results show that microstate intensity for Microstates 4 and 5 were higher in the economic anxiety condition and in turn support the grand average clustering analyses.

Source localization of microstates (sLORETA)

Together, the microstate results demonstrate that the Economic Anxiety condition altered the ERP to error commission. To better characterize these differences, we first conducted sLORETA analyses to source localize the sequence of cortical generators of each microstate in the separate conditions, i.e. Microstates 1, 2, 3, 4, and 5 in the Economic Anxiety condition and Microstates 1, 2, 3, and 6 in the No-Anxiety Control condition.

As seen in Fig. 3, in the No-Anxiety Control condition, Microstate 1 is characterized by dorsal ACC (dACC) and dorsal medial PFC (dmPFC) activation. Given that the timeframe of Microstate 1 is prior to error commission, this pattern of activation fits with an expectancy or early recognition period of an upcoming error (Hajcak et al. 2005). Microstate 2 occurs during the classic ERN component and is characterized by broader midline activation in the ACC and the mPFC. Microstate 3 is characterized by posterior cingulate cortex (PCC) and precuneus activation, as well as lateral PFC activation in the inferior frontal gyrus. Given the links between PCC/

precuneus and self-awareness (e.g. Kjaer et al. 2002; Fransson and Marrelec 2008) and the lateral PFC and regulatory efforts (e.g. Miller and Cohen 2001; Heatherton 2011), this finding is consistent with evidence demonstrating that the Pe, occurring during a matching timeframe, is related to conscious awareness of the error (Nieuwenhuis et al. 2001; Kirschner et al. 2021). Further, this is consistent with research which demonstrates that the lateral PFC is recruited by the ACC after an error in order to implement cognitive control and behavioral adjustments (MacDonald et al. 2000; Kerns et al. 2004). Finally, Microstate 6 is characterized by insula, vmPFC, and lateral PFC activation. This pattern of activation may reflect the negative affective component of error commission (Foti and Hajcak 2008). Overall, the sources of microstates are highly consistent with prior research on ERN and Pe sources (Vocat et al. 2008) and patterns of neural activation after error commission (MacDonald et al. 2000; Miller and Cohen 2001; Botvinick et al. 2004; Yeung et al. 2004; Mansouri et al. 2009). The sequence of activation is also similar across conditions, but the strength of the pattern of activation in the Economic Anxiety condition appears, in general, muted compared to the No-Anxiety Control condition. In addition, Microstate 4, seen only in the Economic Anxiety condition, is characterized by a pattern of weaker activation in general. Microstate 5 is characterized by left anterior insula activation only and not the broader pattern of lateral PFC activation seen in the No-Anxiety Control condition. This suggests that the induction of anxiety interfered with the typical neural processing of errors.

To further probe these underlying neural processes, we next analyzed the conditional effects on the cortical generators in each microstate using sLORETA source localization, directly comparing the common microstates, i.e. 1, 2, and 3. We also compared Microstate 4, found only in the Economic Anxiety condition, to Microstate 3 in the No-Anxiety Control condition as it occurred during the same timeframe, i.e. a Pe. We then compared Microstate 5, found only in the Economic Anxiety condition, to Microstate 6, found only in the No-Anxiety Control condition, as these microstates also occurred during the same time frame, i.e. during a late positivity in the ERP. Significant findings were obtained when comparing Microstate 3 across the Economic-Anxiety and No-Anxiety conditions, as well as between Microstate 4 for the Economic-Anxiety conditions and Microstate 3 for the No-Anxiety condition. Specifically, whole-brain, voxel-by-voxel independent groups t-tests compared error-related sLORETA images from the Microstate 3 timeframe in the Economic Anxiety condition to images from Microstate 3 in the No-Anxiety Control condition, controlling for correct-related sLORETA images. Results revealed that the Economic Anxiety manipulation caused decreased activation (corrected t-value threshold = 3.822) in a cluster of 3 voxels in the left dACC, peak voxel: MNI coordinates

$X = -5$, $Y = 25$, $Z = 30$; $t(91) = 3.83$; uncorrected $P = 0.0002$. The cluster included voxels in Brodmann areas 24 and 32 (see Fig. 4A). When comparing the Microstate 4 timeframe in the Economic Anxiety condition to the Microstate 3 timeframe in the No-Anxiety Control condition, results revealed that the Economic Anxiety manipulation caused decreased activation (corrected t-value threshold = 3.946) in a cluster of 20 voxels in the left PFC, peak voxel: MNI coordinates $(XYZ) = -15$, 45, -5, $t(91) = 4.09$, uncorrected $P = 0.00009$. The cluster included voxels in the middle frontal, superior frontal, and anterior cingulate gyri, in Brodmann areas 10, 11, and 32 (see Fig. 4B). All other comparisons did not cross the whole-brain corrected t-value threshold.

Overall, these results support the disruptive account of anxiety on performance monitoring. Microstate analysis revealed that the grand average ERP in the Economic Anxiety condition was characterized by unique microstates, Microstates 4, which demonstrated a shift to a more limited frontal positivity on the scalp, and Microstate 5, which also demonstrated a shift towards a more anterior and muted positivity. Further, source localization analysis revealed that participants in the Economic Anxiety condition demonstrated reduced dACC and reduced left PFC activation during Microstate 3 and Microstate 4, respectively.

State anxiety: mediation analyses

We next examined if state anxiety mediates the effects of Economic Anxiety on performance monitoring processes. We focused on the main effects demonstrated above, i.e. effects on mean ERN amplitude, dACC activation in Microstate 3, and left PFC activation in Microstate 4. Individual estimates of current density in a 5 mm space around the peak voxel in the dACC cluster during Microstate 3 timeframe and left PFC during the Microstate 4 timeframe were extracted, after errors and correct responses, and respective difference scores were calculated. We conducted 3 separate mediation analyses (PROCESS, Model 4, 5,000 bias-corrected bootstrapped resamples; Hayes 2017) with $X =$ condition (coded as $0 =$ No-Anxiety control, $1 =$ Economic Anxiety) and $M =$ State Anxiety. Results revealed that State Anxiety mediated the effect of the Economic Anxiety manipulation on mean ERN amplitude at FCz, $B = 1.351$, bootstrapped SE $= 0.635$, bootstrapped 95% CI [0.1714, 2.717]; dACC activation to error commission in Microstate 3, $B = -0.426$, bootstrapped SE $= 0.163$, bootstrapped 95% CI [-0.7599, -0.1164]; and, though at 90% CI, left PFC activation to error commission in Microstate 4, $B = -0.4523$, bootstrapped SE $= 0.163$, bootstrapped 90% CI [-0.7599, -0.1164]. In sum, state anxiety mediated the disruptive effect of the Economic Anxiety condition on a muted ERN, reduced dACC activity, and, to a lesser extent, reduced left PFC activity to error commission.
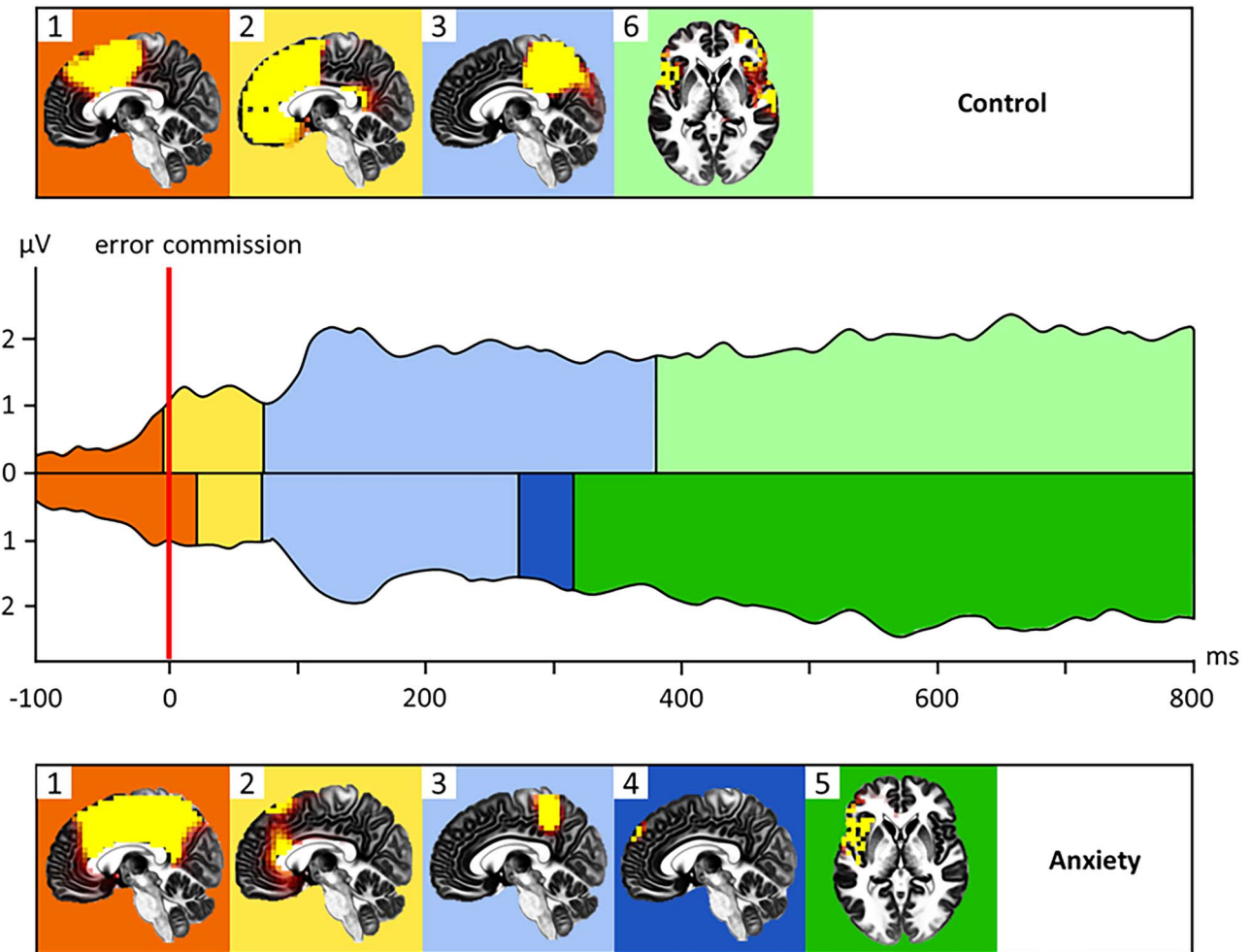
Fig. 3. The sequence of cortical activation networks underlying each microstate in error commission for those in the No-Anxiety Control condition (top) and those in the Economic Anxiety condition (bottom). Microstates 1 and 2 image *t*-value threshold is set at *t*(91) = 6.00. Microstates 3, 5, and 6 image *t*-value threshold is set at *t*(91) = 4.00. Microstate 4 image *t*-value threshold is set at *t*(91) = 3.00 (activation in Microstate 4 did not cross the whole-brain corrected threshold for significance).

Trait anxiety: moderation analyses

To tease apart the impact of state versus trait anxiety on performance monitoring, we conducted moderation analysis of ERN and Pe amplitude by trait anxiety. Further, we conducted whole-brain corrected, source localization analyses of the impact of Condition, trait anxiety (as measured with the BIS scale), and their interaction on the paired contrast between error and correct sLORETA images, at the Microstate 3–4 timeframe (74–379 ms) and the Microstate 5–6 timeframe (379–800 ms), chosen based on the fact that the microstate analyses suggested different sources during these timeframes. For both analyses, we conducted voxel-by-voxel, whole-brain corrected, moderated multiple regression tests of the sLORETA images during these microstate periods (West et al. 1996). The regression model was such that the condition variable and trait anxiety were entered as first-level predictors, and their interaction term entered as a second-level predictor (MATLAB script available upon request).

Moderated sources in Microstates 3–4

Results revealed a significant interaction effect between condition and trait anxiety in 3 voxels in a cluster in the dACC, Brodmann area 24 (see Fig. 6A), beta-value threshold after whole-brain correction for multiple comparisons = 0.377, peak voxel MNI coordinates = 5, 0, 30, *b* = 0.387, corrected *P* = 0.037. Notably, if examined at the corrected threshold of *P* < 0.10 (a yet conservative whole-brain correction), then a cluster of 27 voxels, containing the same region identified above in the conditional effects on cortical generators of Microstate 3 (see above), is also significantly active. To examine the simple effects driving the interaction, we extracted individual estimates of current density in a 5 mm space around the peak voxel in the dACC cluster during Microstate 3 timeframe, after errors and correct responses. This dACC score to errors was entered into a moderated multiple regression analysis using the PROCESS macro in SPSS (Model 1, Hayes 2017), with the dACC score to correct responses entered as a covariate (Fig. 5B). Results showed that at
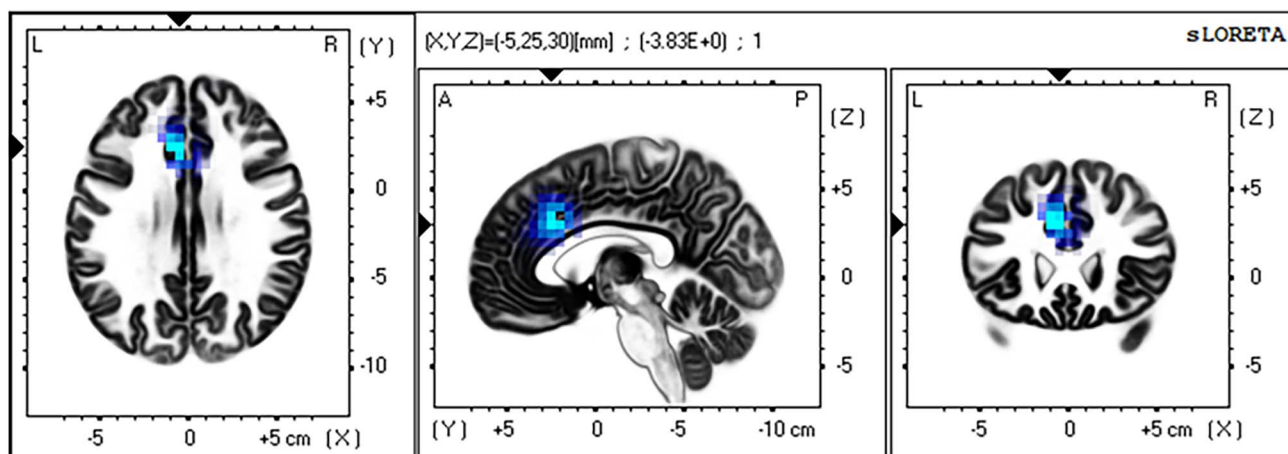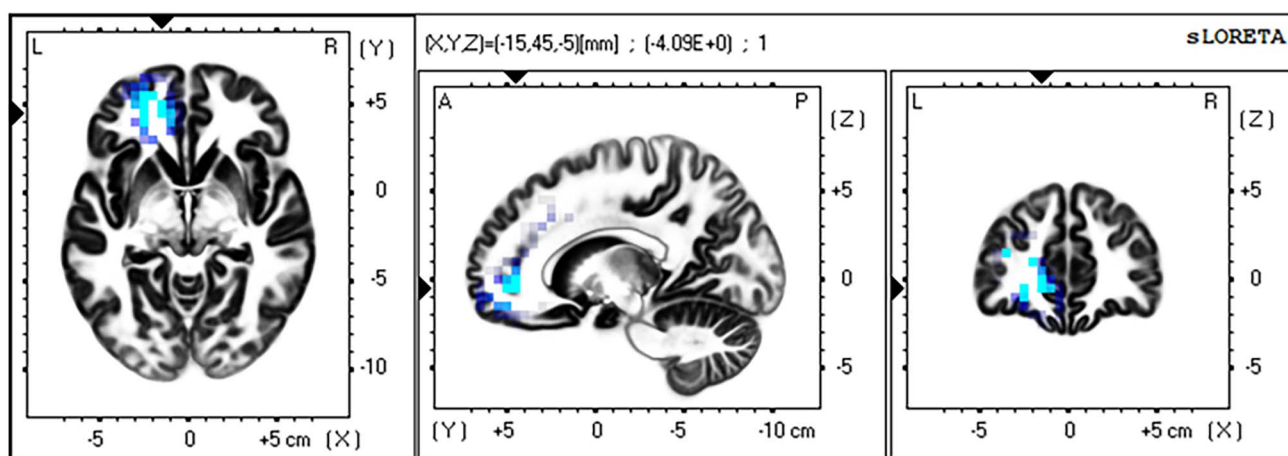
Fig. 4. Source localization (sLORETA) results showing voxels with significantly lower activation in the Economic Anxiety condition compared to the No-Anxiety Control condition. A) Reduced dACC activation during Microstate 3. Significant voxels in blue, critical *t*-value >3.822. Arrows at peak voxel, MNI coordinates = −5, 25, 30, *t*(91) = 3.833. B) Reduced left PFC activation in Microstate 4. Significant voxels in light blue, critical *t*-value>3.776. Arrows at peak voxel, MNI coordinates = 5, 45, −25, *t*(91) = − 4.270.

high levels of trait anxiety (defined as +1SD on the BIS scale, West et al. 1996), people in the Economic Anxiety condition [estimated conditional mean (ECM) = 1.086] showed a significant decrease in dACC current density to error commission compared to those in the No-Anxiety Control condition (ECM = 0.537), *t*(90) = −2.491, *P* = 0.015.

Moderated sources in Microstates 5–6

Results revealed a significant interaction effect between condition and trait anxiety in 2 clusters (beta-value threshold corrected for multiple comparisons = 0.390): a cluster of 6 voxels in the right lateral PFC (middle and inferior frontal lobes), Brodmann areas 6 and 9 (see Fig. 6C and 6D), peak voxel MNI coordinates = 55, 5, 40, *b* = 0.420, corrected *P* = 0.019, and a cluster of 5 voxels in the occipital lobe (cuneus), Brodmann area 18, peak voxel MNI coordinates = 0, −85, 15, *b* = 0.396. Again, to examine the simple effects driving the interaction, we extracted individual estimates of current density in a 5 mm space around the peak voxels in the right lateral prefrontal

cortex (rLPFC) and cuneus clusters during the Microstate 5–6 timeframe. As opposed to the analyses on the dACC, results showed that at high levels of trait anxiety (+1 SD), people in the Economic Anxiety condition (ECM = 1.143) showed a significant increase in rLPFC current density to error commission, compared to those in the No-Anxiety Control condition (ECM = 0.508), *t*(90) = 2.247, *P* = 0.027. Similarly, at high levels of trait anxiety (+1SD), people in the Economic Anxiety condition (ECM = 0.207) showed a significant increase in cuneus current density to error commission, compared to those in the No-Anxiety control condition (ECM = −0.461), *t*(90) = 2.400, *P* = 0.019.

Moderated mediation analyses

Finally, we examined if these cortical sources of conditional effects in Microstates 3–4 and Microstates 5–6 mediate the effect of Economic Anxiety on Stroop performance (i.e. accuracy). First, we conducted moderated mediation analyses (PROCESS, Model 8, 5,000 bias-corrected bootstrapped resamples; Hayes 2017) to
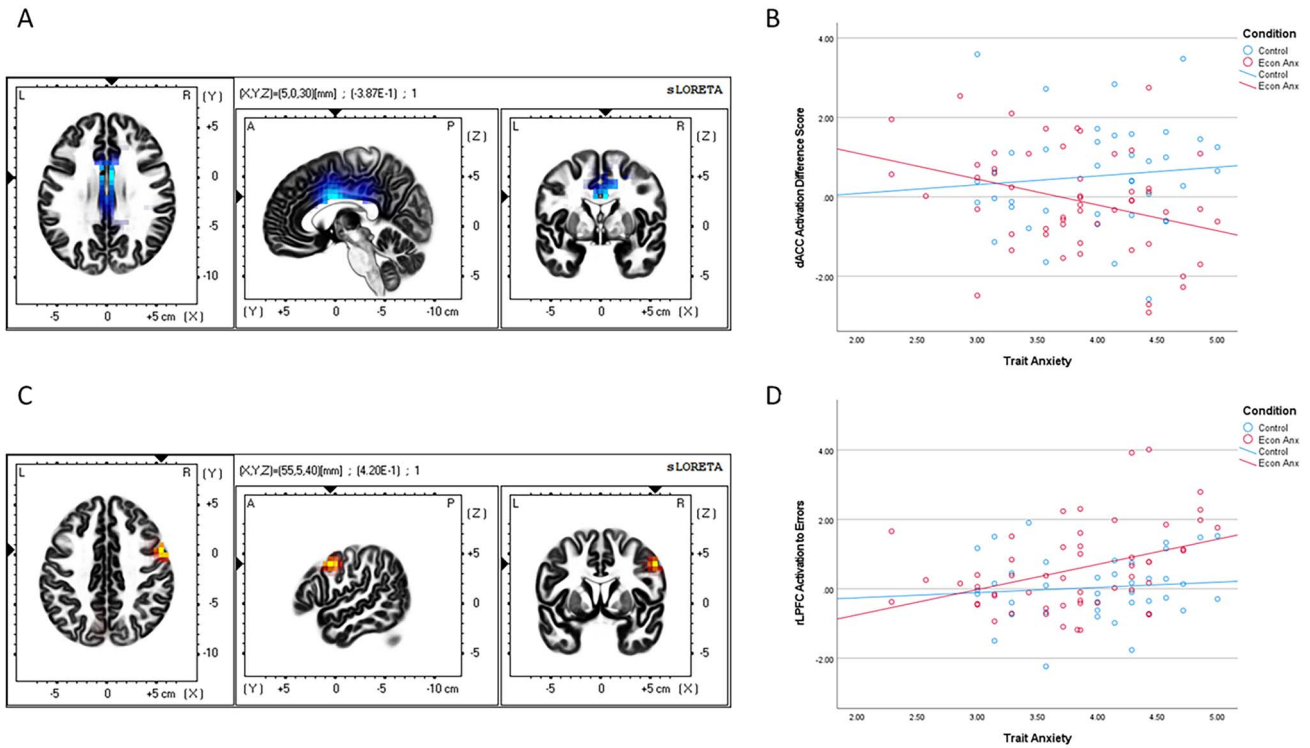
Fig. 5. A) Source localization (sLORETA) results of the interaction between trait anxiety and condition showing voxels with significantly different levels of activation in the dACC. Significant voxels in light blue, critical *b*-value >0.377, arrows at peak voxel, MNI coordinates = 5, 0, 30, *b* = −0.387. B) Scatterplot demonstrating the interaction between trait anxiety and condition on individual estimates of current density in a 5 mm space around the peak voxel in the dACC cluster during Microstate 3 timeframe, after errors minus correct responses. C) Source localization (sLORETA) results of the interaction between trait anxiety and condition showing voxels with significantly different levels of activation in the rLPFC. Significant voxels in yellow, critical *b*-value >0.390, arrows at peak voxel, MNI coordinates = 55, 5, 40, *b* = −0.420. D) Scatterplot demonstrating the interaction between trait anxiety and condition on individual estimates of current density in a 5 mm space around the peak voxel in the rLPFC cluster during Microstate 5–6 timeframe, after errors.
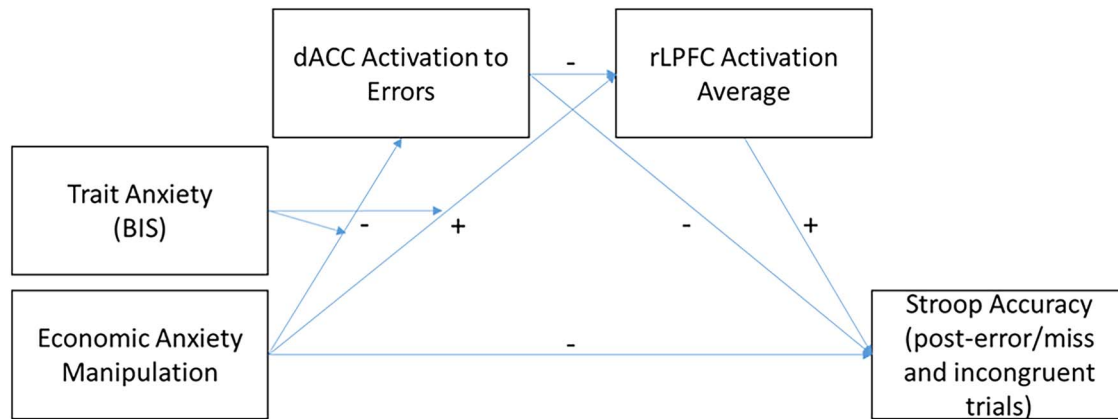
Fig. 6. Moderated mediation model (PROCESS, Model 85, Hayes 2017) demonstrating the indirect paths between condition and Stroop Accuracy. As detailed in the results, among people with high trait anxiety, Economic Anxiety decreased dACC activation, which increased rLPFC activation, which then led to increased accuracy after error and miss trials; PROCESS Model 85, *B* = 0.0115, bootstrapped SE = 0.009, bootstrapped 95% CI [0.0002, 0.0351]; and accuracy on incongruent trials. Signs indicate valence of the indirect effect among people high in trait anxiety.

assess whether dACC activation to error commission mediated the relationship between Economic Anxiety and Stroop accuracy among people with high levels of trait anxiety, X = condition (coded as 0 = No-Anxiety control, 1 = Economic Anxiety), W = BIS subscale score, M = dACC activation to error commission, COV = dACC activation to correct response. Results revealed that,

amongst people with high levels of trait anxiety (+1 SD) only, there was a significant negative indirect effect of the Economic Anxiety manipulation through dACC activation to error commission on accuracy after errors and misses, $B = -0.028$, bootstrapped SE = 0.015, bootstrapped 95% CI [−0.0622, −0.0014]. The indirect effect of accuracy on incongruent trials was significant at the 90% CI level,

$B = −0.030$, bootstrapped $SE = 0.017$, bootstrapped 90% CI [−0.0579, −0.0032]. In short, amongst people high in trait anxiety, the Economic Anxiety condition caused decreased dACC activation to error commission, which then led to decreased accuracy on trials after an error or miss and, to a lesser degree, accuracy on incongruent trials.

We next conducted the same moderated mediation analyses (PROCESS, Model 8, 5,000 bias-corrected bootstrapped resamples; Hayes 2017) to assess whether rLPFC activation to error commission also mediated the relationship between Economic Anxiety and Stroop accuracy among people with high levels of trait anxiety, with $X = $ condition, $W = $ BIS scale score, $M = $ rLPFC activation to error commission. Results revealed that, among people with high levels of trait anxiety (+1 SD) only, there was a significant positive indirect effect of the Economic Anxiety manipulation through rLPFC activation to error commission on accuracy after errors and misses, $B = 0.030$, bootstrapped $SE = 0.018$, bootstrapped 95% CI [0.0039, 0.0745], and accuracy on incongruent trials, $B = 0.029$, bootstrapped $SE = 0.022$, bootstrapped 95% CI [0.0004, 0.0867]. Thus, in opposition to the negative indirect effect associated with dACC activation, among people high in trait anxiety, the Economic Anxiety condition caused increased rLPFC activation to error commission, which then led to increased accuracy on trials after an error or miss and on incongruent trials, suggesting a compensatory function. However, in contrast to the dACC results, this effect is eliminated by inclusion of rLPFC activation to correct responses as a covariate (e.g. accuracy on incongruent trials $B = 0.008$, ns). This suggested that rLPFC activation across both trial types, rather than just rLPFC activation to errors, was important in Stroop accuracy for people high in trait anxiety. Indeed, we entered an average rLPFC activation score computed across all trials into the same moderated mediation analyses, and it revealed the same significant effects: accuracy after errors and misses, $B = 0.025$, bootstrapped $SE = 0.016$, bootstrapped 95% CI [0.0005, 0.0628]; accuracy on incongruent trials, $B = 0.033$, bootstrapped $SE = 0.021$, bootstrapped 95% CI [0.0029, 0.0822].

A moderated mediation analysis with both a dACC activation difference score (to control for correct-related activity) and a rLPFC activation average score entered as serial mediators (PROCESS, Model 85, Hayes 2017) demonstrated a significant indirect effect. Specifically, among people high in trait anxiety, Economic Anxiety caused decreased dACC activation and decreased accuracy. However, the decrease in dACC activation also led to increased rLPFC activation, which then led to "increased" accuracy after errors and misses, $B = 0.016$, bootstrapped $SE = 0.009$, bootstrapped 95% CI [0.0002, 0.0351]; and accuracy on incongruent trials, $B = 0.016$, bootstrapped $SE = 0.012$, bootstrapped 95% CI [0.0006, 0.0464]. Notably, the same analyses are not significant if the rLPFC activation score to error commission is

used. These results thus suggest that although the Economic Anxiety manipulation disrupted dACC-related processing of errors (and Stroop performance), this then led to compensatory activation in the rLPFC, possibly representing increased attentional control across all trials.

Discussion

We set out to investigate how, where, when, and for whom antecedent, task-independent anxiety impacts performance monitoring processes. This research addressed key limitations in prior research. We manipulated real, consequential anxiety prior to the performance monitoring task to rule out confounds such as divided attention or distraction by within-task manipulations. We integrated spatial and temporal EEG information in a microstate approach to precisely sequence the underlying neural network dynamics in error commission. Finally, we measured trait anxiety to examine the interaction between person and context. We sought evidence for either cognitive–disruptive, motivational facilitative, or integrative accounts of anxiety and performance monitoring.

Results showed that, first, the Economic Anxiety condition caused decreased accuracy on incongruent trials and after errors and misses, compared to a control condition. Second, ERP analyses revealed that Economic Anxiety resulted in decreased ERN mean amplitudes after error commission. Third, a group-level microstate analysis after error commission identified unique microstates caused by the Economic Anxiety condition. Microstates 4 and 5 were characterized by reduced fronto-central positivity compared to Microstates 3 and 6 in the control condition, demonstrating a reduced Pe component and late positivity component, respectively. Fourth, source localization revealed that the Economic Anxiety condition caused reduced activation in the dACC during Microstate 3 and in the left PFC during Microstate 4. Fifth, mediation analyses showed that state anxiety mediated the effects of the Economic Anxiety condition on reduced ERN mean amplitude and reduced dACC and left PFC activation to errors. Sixth, moderation analysis demonstrated that participants high in trait anxiety in the Economic Anxiety condition showed decreased activation in the dACC during Microstates 3–4 and increased activation in the rLPFC and cuneus during Microstates 5–6. Finally, moderated mediation analyses revealed that among people high in trait anxiety, although the Economic Anxiety condition disrupted dACC-related processing of errors and disrupted Stroop accuracy, this then led to compensatory activation in the rLPFC and improved Stroop accuracy.

Broadly, the current results support the cognitive view of anxiety and performance monitoring. According to this view, performance monitoring requires control and anxiety is theorized to directly disrupt control (e.g. Eysenck and Derakshan 2011). Consistent with this, here, anxiety was disruptive. An anxious event caused

state anxiety, decreased accuracy in the Stroop task, and decreased activation in a brain region critically involved in performance monitoring processes, the dACC (MacDonald et al. 2000; Bush et al. 2002; Yeung et al. 2004). The dACC has been reliably associated with conflict detection and recruitment of lateral PFC regions for conflict resolution and behavioral modification (MacDonald et al. 2000; Miller and Cohen 2001; Botvinick et al. 2004; Yeung et al. 2004; Mansouri et al. 2009) and has been equated with the comparator function in cybernetic models of self-regulation (Paus 2001; Ito et al. 2003; Shackman et al. 2011; Hauser et al. 2014). Our findings thus complement these models and suggest that antecedent anxiety disrupts performance monitoring processes.

Further, antecedent anxiety primarily disrupted later processes in the ERP after error commission. Though both conditions demonstrated similar appearances of early microstates, scalp activity diverged around 273 ms post-error in Microstate 3, in which the Economic Anxiety condition caused a unique microstate, i.e. Microstate 4. As noted above, Microstates 3 and 4 primarily overlapped with the Pe component typically identified in error-related potentials (Overbeek et al. 2005). The Pe is thought to reflect conscious recognition of errors (Steinhauser and Yeung 2010) and has been source localized in past research to the same dACC region as identified here (Herrmann et al. 2004). Evidence further suggests that the Pe is independent of the ERN and dopaminergic input (Falkenstein et al. 2005), reflecting working memory updating processes akin to a P3b component (Overbeek et al. 2005). As such, the current evidence suggests that antecedent anxiety impacts later, more conscious, regulatory processes after error commission, and leads to performance decrements, particularly during incongruent trials or after mistakes, i.e. when control is most required. We identified similar yet distinct microstates after the Pe, Microstates 5 and 6. These microstates were source localized to vmPFC, insula, and dACC regions, a pattern of activation that suggests saliency or affect-related awareness of the error (Barrett and Simmons 2015; Seeley 2019).

Notably, Microstates 5–6 are not readily apparent as an ERP component at fronto-midline electrodes, though the preceding Microstates 3–4 and Microstates 5–6 were source localized to clearly distinct networks. Broadly, this demonstrates a significant benefit of analyzing the full spatio-temporal EEG information using microstate techniques. To the best of our knowledge, we are the first to apply microstate analysis to ERPs in error commission. This approach integrates the entire spatio-temporal EEG recorded in an ERP, rather than focusing on ERP waveforms measured from a single electrode. Consequently, we were able to sequence and source localize rapid and distinct mental processing steps in error commission to a level not available to traditional imaging methods. We found that neural activation after error commission is typically characterized by 4 distinct microstate networks,

i.e. a pre-error network (Microstate 1), an ERN-related network (Microstate 2), a Pe-related network (Microstate 3), and a late positivity network (Microstate 6; see Fig. 2). The identification of the unique microstate networks 4 and 5 in the Economic Anxiety condition demonstrated that anxiety mutes the activation of neural networks related to both the Pe component and a late positivity component after error commission.

Finally, our examination of trait and state anxiety invites a more nuanced, integrative account, reconciling the competing views on the link between different measures of trait anxiety and performance monitoring. As noted above, past research has found opposing relationships between trait anxiety and performance monitoring (Osinsky et al. 2010; Härpfer et al. 2020; Hsieh et al. 2021; Topor et al. 2021). We found that the association between trait anxiety and performance monitoring was context-dependent. Specifically, our results show that in the control condition, trait anxiety was associated with increased dACC activation after error commission. However, in the Economic Anxiety condition, the relationship with performance monitoring processes flipped as trait anxiety was associated with decreased dACC activation. Under normal circumstances, then, trait anxiety may facilitate heightened vigilance for negative stimuli, including error commission. However, if state anxiety is activated, then trait anxiety may redirect limited attentional resources from the task towards the broader environment. This context-dependent relationship could thus explain the inconsistent findings in past research. That is, the link between trait anxiety and performance monitoring depends on the extent to which participants experience state anxiety during the task. Indeed, past research demonstrates that people high in trait anxiety do not necessarily experience increased state anxiety in any task (Pacheco-Unguetti et al. 2010). Additionally, our moderated mediation model demonstrated a compensatory mechanism. That is, for people high in trait anxiety, disrupted performance monitoring processes appeared to be compensated for through rLPFC activation. This is consistent with a large body of research demonstrating that the rLPFC specifically is involved in regulation and control (Knoch and Fehr 2007).

Overall, we sought to shed light on the uncertain link between anxiety and performance monitoring. This research included 3 key components: (i) a state anxiety manipulation prior to the performance monitoring task to establish a causal link, (ii) microstate analysis to precisely sequence and characterize neural processes in performance monitoring in anxious experiences, and (iii) trait anxiety measures to examine the interaction between trait and state anxiety on performance monitoring. We found that antecedent anxiety was largely disruptive, and the link between trait anxiety and performance monitoring was context-dependent. This has broad implications. It is inevitable that important real-world decisions will be made in the context of anxious experiences, as we all face thoughts of financial

troubles, relational uncertainties, identity, and existential concerns, and, at the time of writing, we remain immersed in the myriad of worries brought on by the COVID-19 pandemic. Future research should examine the extent to which these kinds of anxious experiences and disruptions to performance monitoring processes may be linked to self-regulation and decision-making.

Supplementary Material

Supplementary material can be found at *Cerebral Cortex* online.

Funding

Conflict of interest statement: The authors declare no competing interests.

References

Aarts K, Pourtois G. Anxiety disrupts the evaluative component of performance monitoring: an ERP study. *Neuropsychologia*. 2012:50(7):1286–1296.

Antonova I, van Swam C, Hubl D, Griskova-Bulanova I, Dierks T, Koenig T. Altered visuospatial processing in schizophrenia: an event-related potential microstate analysis comparing patients with and without hallucinations with healthy controls. *Neuroscience*. 2021:479:140–156.

Barrett LF, Simmons WK. Interoceptive predictions in the brain. *Nat Rev Neurosci*. 2015:16(7):419–429.

Botvinick MM, Cohen JD, Carter CS. Conflict monitoring and anterior cingulate cortex: an update. *Trends Cogn Sci*. 2004:8(12):539–546.

Bréchet L, Brunet D, Perogamvros L, Tononi G, Michel CM. EEG microstates of dreams. *Sci Rep*. 2020:10(1):1–9.

Britz J, Michel CM. Errors can be related to pre-stimulus differences in ERP topography and their concomitant sources. *NeuroImage*. 2010:49(3):2774–2782.

Brunet D, Murray MM, Michel CM. Spatiotemporal analysis of multichannel EEG: CARTOOL. *Comput Intell Neurosci*. 2011:2011:813870.

Bush G, Vogt BA, Holmes J, Dale AM, Greve D, Jenike MA, Rosen BR. Dorsal anterior cingulate cortex: a role in reward-based decision making. *Proc Natl Acad Sci*. 2002:99(1):523–528.

Cacioppo S, Balogh S, Cacioppo JT. Implicit attention to negative social, in contrast to nonsocial, words in the Stroop task differs between individuals high and low in loneliness: evidence from event-related brain microstates. *Cortex*. 2015:70:213–233.

Carver CS, Scheier MF. *On the self-regulation of behavior*. Cambridge: Cambridge University Press; 2001

Carver CS, White TL. Behavioral inhibition, behavioral activation, and affective responses to impending reward and punishment: the BIS/BAS scales. *J Pers Soc Psychol*. 1994:67(2):319–333.

da Cruz JR, Favrod O, Roinishvili M, Chkonia E, Brand A, Mohr C, Herzog MH. EEG microstates are a candidate endophenotype for schizophrenia. *Nat Commun*. 2020:11(1):1–11.

de Bock R, Mackintosh AJ, Maier F, Borgward S, Riecher-Rössler A, Andreou C. EEG microstates as biomarker for psychosis in ultra-high-risk patients. *Transl Psychiatry*. 2020:10(1):1–9.

Duval ER, Javanbakht A, Liberzon I. Neural circuits in anxiety and stress disorders: a focused review. *Ther Clin Risk Manag*. 2015:11:115–126.

Eysenck MW, Derakshan N. New perspectives in attentional control theory. *Personal Individ Differ*. 2011:50(7):955–960.

Falkenstein M, Hohnsbein J, Hoormann J, Blanke L. Effects of cross-modal divided attention on late ERP components. II. Error processing in choice reaction tasks. *Electroencephalogr Clin Neurophysiol*. 1991:78(6):447–455.

Falkenstein M, Willemssen R, Hohnsbein J, Hielscher H. Error processing in Parkinson's disease: The error positivity Pe. *J Psychophysiol*. 2005:19(4):305–310.

Foti D, Hajcak G. Deconstructing reappraisal: descriptions preceding arousing pictures modulate the subsequent neural response. *J Cogn Neurosci*. 2008:20(6):977–988.

Fransson P, Marrelec G. The precuneus/posterior cingulate cortex plays a pivotal role in the default mode network: Evidence from a partial correlation network analysis. *NeuroImage*. 2008:42(3):1178–1184.

Gehring WJ, Goss B, Coles MG, Meyer DE, Donchin E. A neural system for error detection and compensation. *Psychol Sci*. 1993:4(6):385–390.

Gratton G, Coles MG, Donchin E. A new method for off-line removal of ocular artifact. *Electroencephalogr Clin Neurophysiol*. 1983:55(4):468–484.

Gray JA, McNaughton N. *The neuropsychology of anxiety: an enquiry into the functions of the septo-hippocampal system*. New York (NY): Oxford University Press; 2000

Hajcak G, Dunning JP, Foti D. Motivated and controlled attention to emotion: time-course of the late positive potential. *Clin Neurophysiol*. 2009:120(3):505–510.

Hajcak G, Foti D. Errors are aversive: defensive motivation and the error-related negativity. *Psychol Sci*. 2008:19(2):103–108.

Hajcak G, McDonald N, Simons RF. Anxiety and error-related brain activity. *Biol Psychol*. 2003:64(1–2):77–90.

Hajcak G, Nieuwenhuis S, Ridderinkhof KR, Simons RF. Error-preceding brain activity: robustness, temporal dynamics, and boundary conditions. *Biol Psychol*. 2005:70(2):67–78.

Härpfer K, Carsten HP, Spychalski D, Kathmann N, Riesel A. Were we erring? The impact of worry and arousal on error-related negativity in a non-clinical sample. *Psychophysiology*. 2020:57(11):e13661.

Hauser TU, Iannaccone R, Stämpfli P, Drechsler R, Brandeis D, Walitza S, Brem S. The feedback-related negativity FRN revisited: new insights into the localization, meaning and network organization. *NeuroImage*. 2014:84:159–168.

Hayes AF. *Introduction to mediation, moderation, and conditional process analysis: a regression-based approach*. New York (NY): The Guilford Press; 2017

Heatherton TF. Neuroscience of self and self-regulation. *Annu Rev Psychol*. 2011:62(1):363–390.

Herrmann MJ, Römmler J, Ehlis AC, Heidrich A, Fallgatter AJ. Source localization (LORETA) of the error-related-negativity (ERN/Ne) and positivity (Pe). *Cogn Brain Res*. 2004:20(2):294–299.

Hsieh MT, Lu H, Lin CI, Sun TH, Chen YR, Cheng CH. Effects of trait anxiety on error processing and post-error adjustments: an event-related potential study with stop-signal task. *Front Hum Neurosci*. 2021:15:290.

Ito S, Stuphorn V, Brow JW, Schall JD. Performance monitoring by the anterior cingulate cortex during saccade countermanding. *Science*. 2003:302(5642):120–122.

Jackson F, Nelson BD, Proudfit GH. In an uncertain world, errors are more aversive: evidence from the error-related negativity. *Emotion.* 2015:15(1):12–16.

Kerns JG, Cohen JD, MacDonald AW III, Cho RY, Stenger VA, Carter CS. Anterior cingulate conflict monitoring and adjustments in control. *Science.* 2004:303(5660):1023–1026.

Khateb A, Michel CM, Pegna AJ, Landis T, Annoni JM. New insights into the Stroop effect: a spatiotemporal analysis of electric brain activity. *Neuroreport.* 2000:11(9):1849–1855.

Kirschner H, Humann J, Derrfuss J, Danielmeier C, Ullsperger M. Neural and behavioral traces of error awareness. *Cogn Affect Behav Neurosci.* 2021:21(3):573–591.

Kjaer TW, Nowak M, Lou HC. Reflective self-awareness and conscious states: PET evidence for a common midline parietofrontal core. *NeuroImage.* 2002:17(2):1080–1086.

Knoch D, Fehr E. Resisting the power of temptations: the right prefrontal cortex and self-control. *Ann N Y Acad Sci.* 2007:1104(1):123–134.

Ladouceur CD, Dahl RE, Birmaher B, Axelson DA, Ryan ND. Increased error-related negativity ERN in childhood anxiety disorders: ERP and source localization. *J Child Psychol Psychiatry.* 2006:47(10):1073–1082.

Laxton AW, Tang-Wai DF, McAndrews MP, Zumsteg D, Wennberg R, Keren R, Lozano AM. A phase I trial of deep brain stimulation of memory circuits in Alzheimer's disease. *Ann Neurol.* 2010:68(4):521–534.

Leota J, Kleinert T, Tran A, Nash K. Neural signatures of heterogeneity in risk-taking and strategic consistency. *Eur J Neurosci.* 2021a:54(9):7214–7230.

Leota J, Nash K, McGregor I. Reactive risk-taking: anxiety regulation via approach motivation increases risk-taking behavior. *Personal Soc Psychol Bull.* 2021b:014616722110596.

MacDonald AW, Cohen JD, Stenger VA, Carter CS. Dissociating the role of the dorsolateral prefrontal and anterior cingulate cortex in cognitive control. *Science.* 2000:288(5472):1835–1838.

Mansouri FA, Tanaka K, Buckley MJ. Conflict-induced behavioural adjustment: a clue to the executive functions of the prefrontal cortex. *Nat Rev Neurosci.* 2009:10(2):141–152.

McNaughton N, Corr PJ. A two-dimensional neuropsychology of defense: fear/anxiety and defensive distance. *Neurosci Biobehav Rev.* 2004:28(3):285–305.

Ménétré E, Laganaro M. The temporal dynamics of the Stroop effect from childhood to young and older adulthood. *bioRxiv.* 2021. Available from: https://doi.org/10.1101/2021.08.13.456209

Michael JA, Wang M, Kaur M, Fitzgerald PB, Fitzgibbon BM, Hoy KE. EEG correlates of attentional control in anxiety disorders: a systematic review of error-related negativity and correct-response negativity findings. *J Affect Disord.* 2021:291:140–153.

Michel CM, Koenig T. EEG microstates as a tool for studying the temporal dynamics of whole-brain neuronal networks: a review. *NeuroImage.* 2018:180(Pt B):577–593.

Miller EK, Cohen JD. An integrative theory of prefrontal cortex function. *Annu Rev Neurosci.* 2001:24(1):167–202.

Mobascher A, Brinkmeyer J, Warbrick T, Musso F, Wittsack HJ, Stoermer R, Winterer G. Fluctuations in electrodermal activity reveal variations in single trial brain responses to painful laser stimuli—a fMRI/EEG study. *NeuroImage.* 2009:44(3):1081–1092.

Moran TP, Bernat EM, Aviyente S, Schroder HS, Moser JS. Sending mixed signals: worry is associated with enhanced initial error processing but reduced call for subsequent cognitive control. *Soc Cogn Affect Neurosci.* 2015:10(11):1548–1556.

Moser JS, Hajcak G, Simons RF. The effects of fear on performance monitoring and attentional allocation. *Psychophysiology.* 2005:42(3):261–268.

Moser J, Moran T, Schroder H, Donnellan B, Yeung N. On the relationship between anxiety and error monitoring: a meta-analysis and conceptual framework. *Front Hum Neurosci.* 2013:7:466.

Nash K, Kleinert T, Leota J, Scott A, Schimel J. Resting-state networks of believers and non-believers: an EEG microstate study. *Biol Psychol.* 2022:108283:108283.

Nash K, Leota J, Tran A. Neural processes in antecedent anxiety modulate risk-taking behavior. *Sci Rep.* 2021:11(1):2637.

Nash K, Tran A, Leota J, Scott A. Economic threat heightens conflict detection: sLORETA evidence. *Soc Cogn Affect Neurosci.* 2020:15(9):981–990.

Nichols TE, Holmes AP. Nonparametric permutation tests for functional neuroimaging: a primer with examples. *Hum Brain Mapp.* 2002:15(1):1–25.

Nieuwenhuis S, Ridderinkhof KR, Blom J, Band GP, Kok A. Error-related brain potentials are differentially related to awareness of response errors: evidence from an antisaccade task. *Psychophysiology.* 2001:38(5):752–760.

Olbrich S, Mulert C, Karch S, Trenner M, Leicht G, Pogarell O, Hegerl U. EEG-vigilance and BOLD effect during simultaneous EEG/fMRI measurement. *NeuroImage.* 2009:45(2):319–332.

Olvet DM, Hajcak G. The error-related negativity ERN and psychopathology: toward an endophenotype. *Clin Psychol Rev.* 2008:28(8):1343–1354.

Osinsky R, Alexander N, Gebhard H, Hennig J. Trait anxiety and dynamic adjustments in conflict processing. *Cogn Affect Behav Neurosci.* 2010:10(3):372–381.

Overbeek TJ, Nieuwenhuis S, Ridderinkhof KR. Dissociable components of error processing: on the functional significance of the Pe vis-à-vis the ERN/Ne. *J Psychophysiol.* 2005:19(4):319–329.

Pacheco-Unguetti AP, Acosta A, Callejas A, Lupiáñez J. Attention and anxiety: different attentional functioning under state and trait anxiety. *Psychol Sci.* 2010:21(2):298–304.

Pasion R, Paiva TO, Fernandes C, Almeida R, Barbosa F. ERN modulation under sustained threat: a pre-registered report. *J Res Pers.* 2018:77:137–146.

Paus T. Primate anterior cingulate cortex: where motor control, drive and cognition interface. *Nat Rev Neurosci.* 2001:2(6):417–424.

Proudfit GH, Inzlicht M, Mennin D. Anxiety and error monitoring: the importance of motivation and emotion. *Front Hum Neurosci.* 2013:7:636.

Pujol J, López A, Deus J, Cardoner N, Vallejo J, Capdevila A, Paus T. Anatomical variability of the anterior cingulate gyrus and basic dimensions of human personality. *NeuroImage.* 2002:15(4):847–855.

Rohde KB, Fey W, Moggi F, Koenig T, Luedi I, Duppenthaler L, Stein M. Deficient processing of alcohol cues in the addicted brain: evidence from event-related potential microstates. *Clin Neurophysiol.* 2020:131(9):2224–2235.

Ruggeri P, Meziane HB, Koenig T, Brandner C. A fine-grained time course investigation of brain dynamics during conflict monitoring. *Sci Rep.* 2019:9(1):1–11.

Schiller B, Gianotti LR, Baumgartner T, Nash K, Koenig T, Knoch D. Clocking the social mind by identifying mental processes in the IAT with electrical neuroimaging. *Proc Natl Acad Sci.* 2016:113(10):2786–2791.

Schiller B, Heinrichs M, Beste C, Stock AK. Acute alcohol intoxication modulates the temporal dynamics of resting electroencephalography networks. *Addict Biol.* 2021:26(6).

Schiller B, Kleinert T, Teige-Mocigemba S, Klauer KC, Heinrichs M. Temporal dynamics of resting EEG networks are associated with prosociality. *Sci Rep*. 2020:10(1):1–10.

Schiller B, Koenig T, Heinrichs M. Oxytocin modulates the temporal dynamics of resting EEG networks. *Sci Rep*. 2019:9(1):1–9.

Seeley WW. The salience network: a neural system for perceiving and responding to homeostatic demands. *J Neurosci*. 2019:39(50):9878–9882.

Seow TXF, Benoit E, Dempsey C, Jennings M, Maxwell A, McDonough M, Gillan CM. A dimensional investigation of error-related negativity ERN and self-reported psychiatric symptoms. *Int J Psychophysiol*. 2020:158:340–348.

Shackman AJ, Salomons TV, Slagter HA, Fox AS, Winter JJ, Davidson RJ. The integration of negative affect, pain and cognitive control in the cingulate cortex. *Nat Rev Neurosci*. 2011:12(3): 154–167.

Smart CM, Segalowitz SJ. Respond, don't react: the influence of mindfulness training on performance monitoring in older adults. *Cogn Affect Behav Neurosci*. 2017:17(6): 1151–1163.

Steinhauser M, Yeung N. Decision processes in human performance monitoring. *J Neurosci*. 2010:30(46):15643–15653.

Topor M, Opitz B, Leonard HC. Error-related cognitive control and behavioral adaptation mechanisms in the context of motor functioning and anxiety. *Front Hum Neurosci*. 2021:15:9.

Vocat R, Pourtois G, Vuilleumier P. Unavoidable errors: a spatio-temporal analysis of time-course and neural sources of evoked potentials associated with error processing in a speeded task. *Neuropsychologia*. 2008:46(10):2545–2555.

West SG, Aiken LS, Krull JL. Experimental personality designs: analyzing categorical by continuous variable interactions. *J Pers*. 1996:64(1):1–48.

Yeung N, Botvinick MM, Cohen JD. The neural basis of error detection: conflict monitoring and the error-related negativity. *Psychol Rev*. 2004:111(4):931–959.

Zumsteg D, Friedman A, Wieser HG, Wennberg RA. Propagation of interictal discharges in temporal lobe epilepsy: correlation of spatiotemporal mapping with intracranial foramen ovale electrode recordings. *Clin Neurophysiol*. 2006:117(12): 2615–2626.